DESIGN AND EXPERIMENTAL EVALUATION OF A CELL-WHEEL SEED-METERING DEVICE FOR RAPESEED BLANKET SEEDLING PRODUCTION
/
窝眼轮式油菜毯状苗育苗排种器的设计与试验

Yaodong WU[1], Jing LUO[2], Qing TANG[1,2], Jixuan WANG[2], Qun LI[1], Meng BAI[2], Jinhui CHEN[2], Tong WU[1]
[1] Jiangsu Yunma Agricultural Machinery Manufacturing Co., Ltd., Yancheng, 224100, China
[2]Nanjing Institute of Agricultural Mechanization, Ministry of Agriculture and Rural Affairs, Nanjing, 210014, China;
Corresponding author: Qing TANG
Tel: +86.15366092914; E-mail: tangqing01@caas.cn
DOI: https://doi.org/10.35633/inmateh-79-64

***Keywords**: rapeseed blanket seedlings; cell-wheel seed-metering device; seed-filling mechanics; response surface optimization; qualified seed-metering rate*

ABSTRACT
To address the low operating efficiency and uneven seeding associated with conventional seedling-production seeders, a cell-wheel seed-metering device was developed specifically for rapeseed blanket seedling production. The key components of the device were designed, and its seed-filling and seed-metering characteristics were analyzed. Using 'Ningza 1838' rapeseed as the test material, single-factor tests and multifactor response surface experiments were conducted. Seed-metering wheel rotational speed, seedling-tray conveying speed, and seed-box opening size were selected as the test factors, while the qualified seed-metering rate and missed-hill rate were used as the performance indicators. The results showed that the factors influencing the performance indicators, in descending order, were seed-box opening size, seedling-tray conveying speed, and seed-metering wheel rotational speed. The optimal parameter combination consisted of a seed-metering wheel rotational speed of 9.16 r·min⁻¹, a seedling-tray conveying speed of 0.45 m·s⁻¹, and a seed-box opening size of 22.80 mm. Under these conditions, the bench test yielded a qualified seed-metering rate of 94.41% and a missed-hill rate of 1.49%. These values were consistent with the predicted results, with deviations of less than 0.5 percentage points.

摘要
针对现有油菜育苗排种器作业效率低、播种均匀性差等问题，设计了一种窝眼轮式油菜育苗排种器，分析了充种与排种过程的力学特性与影响因素。以宁杂 1838 油菜种子为试验材料，以排种轮转速、秧盘输送速度、种箱开度为试验因素，以播种合格率及空穴率为性能评价指标，开展单因素和多因素响应面试验。结果表明：影响评价指标的主次顺序为种箱开度、秧盘输送速度和排种轮转速，最优参数组合为排种轮转速 9.16r·min^{-1}，秧盘输送速度 0.45m·s^{-1}，种箱开度 22.80 mm，在最优参数下的该条件下台架试验播种合格率为 94.41%，空穴率为 1.49%，与预测值误差小于 0.5 个百分点。

INTRODUCTION
Rapeseed is an important oil crop in China, with a planting area of more than 6.5 million hm² (*Wu et al., 2024; Deng.,2023).* Its cultivation includes seedling transplanting and direct seeding. Compared with direct seeding, seedling transplanting can shorten the growth period in the field and effectively alleviate the contradiction of crop rotation, so it has been widely valued (*Lin et al.,2023*). Cultivating qualified and robust rapeseed blanket seedlings is the prerequisite for high-quality transplanting, and the quality of seedling sowing is crucial. The seed-metering device is the core component of the seedling-production system, and its performance directly influences seedling quality (*Wang et al.,2023*). Due to the characteristics of small size, light weight and large particle size variation of rapeseed seeds, problems such as missed seeding, multiple seeding, off-center seed placement and localized seed accumulation can readily occur during operation (*Cong J., 2014*), leading to an increase in the empty-cell rate and a decrease in the qualified rate. Therefore, developing a precision seeding device suitable for rapeseed blanket seedling production is important for improving seedling quality and, ultimately, rapeseed yield.

Seeding devices can be divided into pneumatic and mechanical types. Pneumatic precision seeders usually realize seed filling and metering by negative pressure adsorption or positive pressure ejection. They are characterized by strong single-seed separation ability and good adaptability to seed shape differences, and can theoretically maintain high precision at a relatively high operating speed (*Cao et al., 2021; Li et al., 2020*). Most studies focus on the optimization of seed-airflow dynamics.

Singh R.C et al. (2006) optimized the structure and operating parameters of pneumatic seeders for sowing different seeds such as mustard and peanut. *Albasheer et al. (2024)* designed a cylindrical pneumatic centralized seed metering device, which was suitable for rice, wheat and rapeseed through a double-cell wheel structure, with a field emergence rate of 88% and a coefficient of variation of 3.44%. *Akhalaya et al. (2021)* adopted a synchronous staggered double-disc and double-nozzle seed cleaning structure to solve the contradiction between seed adhesion and missed seeding, enabling compact double-row sowing. *Liao et al. (2018)* explored the influencing factors of seed suction performance of pneumatic precision seeders for small-sized seeds through seed suction and migration tests. *Li et al. (2019)* used EDEM numerical simulation to study the influence laws of various factors on seed population disturbance. *Gao et al. (2022)* proposed a conical hole seed disc, which was verified by theory, simulation and experiments to improve the performance of rapeseed precision seeders, significantly increasing the qualification index and reducing the rates of repeated and missed seeding.

However, despite these advances, pneumatic systems still face inherent limitations: the whole machine structure is complex, manufacturing and maintenance costs remain high, and the small size of rapeseed grains makes seeding consistency susceptible to air pressure fluctuations. Moreover, pneumatic seeders require dedicated air supply and vacuum systems, which increase energy consumption and limit their application in small-scale and hilly farming operations. Mechanical precision seeders generally achieve seed filling and metering through mechanical force. Typical types include grooved wheel, finger clamp, disc, hole wheel, and cell wheel type (*Liu Y et al., 2019; Wang et al., 2022; Li et al., 2025*). Most studies focus on device structure innovation and size optimization. *Maleki et al. (2006)* studied and evaluated the seed distribution uniformity of a multi-screw conveyor as a seeding device for grain drills, and found that its performance was superior to that of the traditional fluted roller device. *Karayel et al. (2022)* established a model between seed physical properties and optimal vacuum degree based on artificial neural network, with a prediction accuracy $R^2 > 0.99$, providing a basis for pressure regulation on demand. *Singh et al. (2005)* took cotton seeds as the object and obtained that the combination of 120° conical holes, 2 kPa vacuum degree and 0.42 m/s linear velocity could achieve a single-seed rate of 94.7%, providing a reference for the optimization of small seed seeders. *Lei et al. (2020)* analyzed the influences of cell length, cross-section size and cell depth on rapeseed filling performance through simulation, and proposed involute-shaped cells suitable for 1–3 seeds per hill of rapeseed. *Zhang et al. (2020)* analyzed the working process of the seeder, determined the spoon-wheel combination and the main parameters such as the size, installation number, installation inclination angle of the spoon-type cells and the rotating speed of the spoon wheel, and designed a rapeseed precision hill-seeding metering device with notched rectangular spoon-type cells. *Xing et al. (2019)* proposed a structure with staggered double circles of cells for rapeseed and three circles for wheat, as well as oblique conical cells by establishing a mechanical model of the sowing process. Among mechanical seeders, the cell wheel type stands out for its simple structure, ease of processing, and convenient seed cleaning, making it particularly suitable for small-seed crops like rapeseed.

However, a critical review of the existing literature reveals a significant scientific gap: most studies on cell wheel seeders for rapeseed have focused either on conventional direct seeding applications or on generalized seed metering for multiple crop types, with limited attention to the specific requirements of blanket seedling nursery production. The nursery seeding process imposes distinct demands—including precise control of 2–3 seeds per cell, compatibility with high-speed seedling tray conveying, and stable performance under continuous operation—that are not adequately addressed by existing designs. Furthermore, systematic investigations into the interactive effects of key operational parameters (metering wheel speed, tray conveying speed, and seed box opening) on seeding performance for blanket seedling applications remain scarce, and the underlying seed-filling mechanics have not been fully characterized for this specific context.

To address this gap, this study developed a novel cell-wheel seed-metering device specifically for rapeseed blanket seedling production. The cylindrical cell structure is simple, easy to manufacture, and convenient to clean. Although its seed-guiding performance is slightly inferior to that of conical or hemispherical cells, reliable seed filling and low seed damage can be achieved by optimizing the cell depth-to-diameter ratio. The principal innovations of the proposed device are threefold: (1) it is the first cell-wheel seed-metering device to be systematically designed and optimized for the nursery seeding stage of rapeseed blanket seedling production, with the cell geometry and arrangement tailored to the agronomic requirement of 2–3 seeds per tray cell; (2) it incorporates a synchronized seed-cleaning brush and seed-cleaning blade, enabling continuous removal of excess seeds without causing seed damage or cell blockage and thereby addressing a common failure mode in mechanical metering devices for small seeds; and (3) through comprehensive mechanical analyses of the seed-filling and seed-discharging processes, it establishes a theoretical basis for parameter optimization by directly linking operating parameters to seed-metering performance indices.

The specific objectives of this study were: (i) to design and fabricate a cell-wheel seed-metering device for rapeseed blanket seedling production, with the key structural parameters determined through theoretical analyses of the seed-filling and seed-metering processes; (ii) to investigate the effects of seed-metering wheel rotational speed, seedling-tray conveying speed, and seed-box opening size on the qualified seed-metering rate and empty-cell rate through single-factor and response surface experiments; and (iii) to determine the optimal combination of operating parameters through multi-objective optimization and validate the results through bench tests. The findings provide a reference for the structural optimization and parameter matching of seed-metering devices for rapeseed blanket seedling production and offer technical support for the development of precision seeding equipment for other small-seeded crops.

MATERIALS AND METHODS

Structure and Operating Principle of the Seed-Metering Device

The principal components of the rapeseed blanket-seedling seed-metering device include a cell-wheel seed meter, seed-cleaning brush, seed box, seed-guide plate, seed-box opening adjustment plate, seed-retaining plate, seed-cleaning blade, and continuously variable-speed motor (Fig. 1). The main technical parameters are listed in Table 1. The operating principle is as follows. Under the action of gravity, rapeseed seeds in the seed box pass through the seed outlet and enter the seed-filling zone under the guidance of the seed-guide plate. Driven by the motor, the seed-metering wheel and seed-cleaning brush rotate synchronously. Seeds enter the cells of the metering wheel under the combined effects of gravity and pressure from the seed mass. As the seed-metering wheel rotates, the seeds retained in the cells pass through the seed-retaining zone. The seed-cleaning brush continuously removes excess seeds from the cells and returns them to the seed-filling zone. The retained seeds continue to rotate with the metering wheel while being held in place by the seed-retaining plate. When the cells reach the seed-discharging zone, the seeds are no longer constrained by the seed-retaining plate and are discharged under the combined effects of gravity and the seed-cleaning blade. They then fall uniformly into the cells of the seedling tray carried by the conveyor belt, thereby completing the seed-metering process.

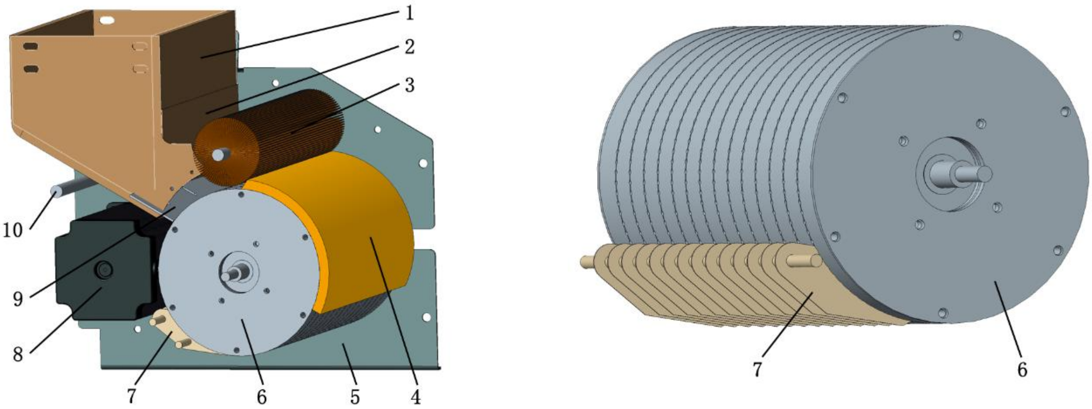

a) *b)*

Fig. 1 - Structure of the cell-wheel seed-metering device

a) Seed-metering device assembly; b) Cell-wheel

1.Seed box; 2. Seed-box opening adjustment plate; 3. Seed-cleaning brush; 4. Seed-retaining plate; 5. Housing; 6. Cell-wheel; 7. Seed-cleaning blade; 8. Continuously variable-speed motor; 9. Seed-guide plate; 10. Support rod

Table 1

Main parameters of the seed-metering device

No.	Parameter	Value
1	Seed-metering device type	Cell-wheel type
2	Cell shape	Cylindrical
3	Number of cells per circumferential row	90
4	Cell diameter [mm]	3
5	Cell depth [mm]	5
6	Center-to-center spacing between adjacent cells [mm]	20
7	Seed-metering wheel diameter [mm]	160
8	Seed-metering wheel circumference [mm]	512
9	Seed-metering wheel width [mm]	303
10	Number of axial cell rows	14

No.	Parameter	Value
11	Seeding rate [g·tray^{-1}]	3.28 ~ 5.33
12	Seeding rate adjustment method	Stepless adjustment

Figure 2 shows the cell arrangement on the developed surface of the seed-metering wheel, with the principal dimensions defined in Table 1. In Fig. 2, a is the circumferential spacing between adjacent cells, b is the axial center-to-center spacing between adjacent cells, c is the cell diameter, d is the width of the seed-cleaning groove, e is the depth of the seed-cleaning groove, and f is the cell depth. The number of axial cell rows was set to 14 based on the seedling-pickup cycle of the rapeseed blanket seedling transplanter *(Jiang et al., 2024; Wu et al., 2020)*.

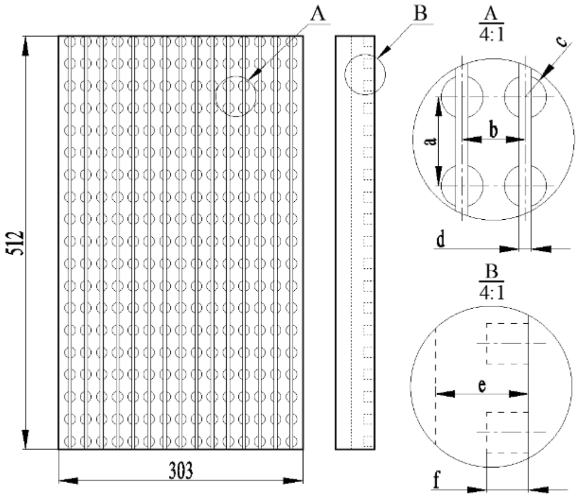

Fig. 2 - Cell arrangement on the developed surface of the seed-metering wheel

Analysis of the Seed-Filling Process of the Seed-Metering Device

Cell geometry is a critical design parameter that directly affects seed filling, retention, and cleaning performance. In this study, cylindrical cells were selected based on the physical properties of rapeseed, manufacturing feasibility, and operational requirements. Rapeseed seeds are approximately spherical, with diameters of 2–3 mm and relatively smooth surfaces. The axisymmetric geometry of a cylindrical cell therefore provides uniform radial clearance around the seeds, facilitating entry into the cell and stable retention during wheel rotation. Compared with conical or hemispherical cells, cylindrical cells offer several advantages.

First, their simple geometry facilitates conventional machining or injection molding, helping ensure dimensional consistency and reduce manufacturing costs. Second, the straight cell walls reduce the wedging effect that may occur in tapered cells when slightly oversized seeds enter the cavity, thereby decreasing the risk of seed damage and cell blockage. Third, the uniform cross-section throughout the cell depth supports stable filling with the agronomically required 2–3 seeds per cell. The seeds can stack naturally within the cylindrical cavity rather than being forced into a narrowing space. Spoon-shaped or elliptical cells may improve single-seed metering in precision direct-seeding applications.

However, their irregular inlet geometry may restrict seed entry, while localized dead zones may retain seed dust and debris, potentially increasing the missed-seeding rate during continuous nursery operation. Cylindrical cells also facilitate seed cleaning. The seed-cleaning brush can sweep smoothly across the flat cell openings without snagging, while the seed-cleaning blade can dislodge seeds that remain partially retained in the cells. These functions may be less reliable with non-axisymmetric cell geometries. The selected cell diameter of 3 mm and depth of 5 mm were determined according to the rapeseed diameter of 2–3 mm, the target seeding rate, and the design requirements of cell-wheel seed-metering devices. This combination provides sufficient cell volume to accommodate 2–3 seeds while reducing the empty-cell rate and limiting excessive multiple seeding beyond the agronomic requirement.

When the cell wheel rotates into the seed-filling zone, rapeseed seeds enter the cells, thereby completing the seed-filling process, as shown in Fig. 3(a). The time available for seeds to enter the cells is a key factor affecting the filling performance of the seed-metering wheel. Therefore, to analyze the seed-filling process and optimize filling performance, the forces acting on an individual rapeseed seed were analyzed, and the required filling time was subsequently calculated.

Rapeseed seeds were simplified as spherical particles with uniform mass distribution and regular arrangement. The vertical pressure acting on a seed was assumed to result only from the weight of the overlying seed layer; lateral pressure, vibration, and other disturbances were neglected. During seed filling, a seed is mainly subjected to its weight G, centrifugal force F_2, Coriolis force F_3, the compressive force exerted by adjacent seeds F_1, the normal reaction force of the cell wall N, the friction force between the seed and the cell wall f_2, and the interseed friction force f_1. A coordinate system was established with the seed center as the origin, the direction normal to the cross-section of the seed-metering wheel as the x-axis, and the tangential direction as the y-axis, as shown in Fig. 3(b). The equations of motion are expressed as follows:

$$\begin{cases} ma_x = (F_1 + G)\cos\theta + f_1 \sin\theta - F_3 - F_2 - N \\ ma_y = f_2 + f_1 \cos\theta - (F_1 + G) f_1 \sin\theta \\ F_2 = mr\varpi^2 \\ F_3 = 2mv_r\varpi \\ f_1 = \mu_1 F_1 \\ f_2 = \mu_2 F_2 \\ G = mg \end{cases} \tag{1}$$

where: m is mass of a single seed, [kg]; θ is the acute angle between the direction of the centrifugal force acting on the seed and the vertical direction, [rad]; a_x is the normal acceleration of the seed, [m/s²]; a_y is the tangential acceleration of the seed, [m/s²]; r is the distance from the seed centroid to the center of the seed-metering wheel, [m]; ω is the angular velocity of the seed-metering wheel, [rad/s]; μ_1 is the coefficient of friction between seeds; μ_2 is the coefficient of friction between the seed and the cell wall.

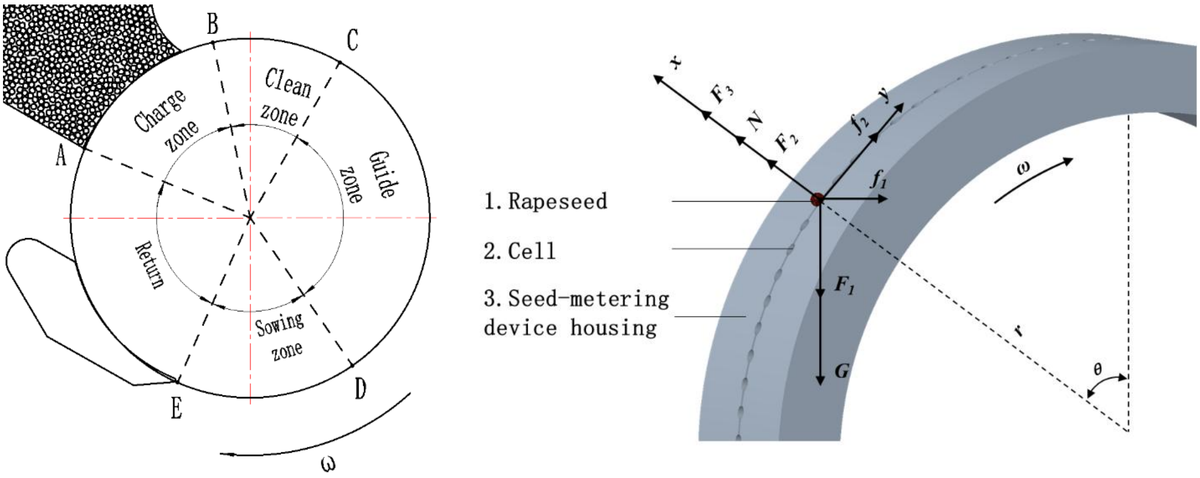

a) b)

Fig. 3 - Seed-filling process and force analysis
a) Schematic of the seed-filling process; b) Free-body diagram of a single seed during seed filling

Rearranging Equation (1) yields:

$$\begin{cases} a_x = \frac{(mg+F_1)\cos\theta + \mu_1 F_1 \sin\theta - N}{m} - 2v_r\varpi - r\varpi^2 \\ a_y = \frac{\mu_2 F_2 + \mu_1 F_1 \cos\theta - (F_1 + mg)\sin\theta}{m} \end{cases} \tag{2}$$

According to the analysis of the seed filling process of a single seed, the following relationship exists between the normal displacement h of the seed centroid along the cross-section of the seed metering wheel (i.e., the hole depth) and its tangential acceleration a_x: According to the force analysis of a single seed during the filling process, the normal displacement h of the seed centroid along the cross-section of the seed-metering wheel, corresponding to the cell depth, is related to the normal acceleration a_x as follows:

$$h = \frac{1}{2} a_x t^2 \tag{3}$$

where: t is the time required for the seed to enter the cell, [s].

Combining Equations (2) and (3), the seed-filling time t (s) is obtained as:

$$t = \sqrt{\frac{2hm}{(mg+F_1)\cos\theta + \mu_1 F_1 \sin\theta - N - 2v_r\varpi m - mr\varpi^2}} \tag{4}$$

To improve seed-filling performance, the time required for seeds to enter the cells should be minimized. Because the angular range θ of the seed-filling zone is fixed, Equation (4) indicates that the filling time t is primarily affected by parameters such as seed mass m, cell depth h, and the interseed friction coefficient μ_1. The diameter of seeds from common rapeseed cultivars is approximately 2.5 mm. Based on the design criteria for cell-wheel seed-metering devices *(Cong, 2014)*, the cell diameter was set to 3 mm and the cell depth h to 5 mm.

Analysis of the Seed-Discharging Process of the Seed-Metering Device

After entering the seed-discharging zone, the seeds are no longer constrained by the cells or the seed-retaining plate. Under the action of gravity, they leave the cells with an initial velocity determined by the rotational motion of the seed-metering wheel and subsequently undergo projectile motion. The seed-discharge trajectory is shown in Fig. 4.

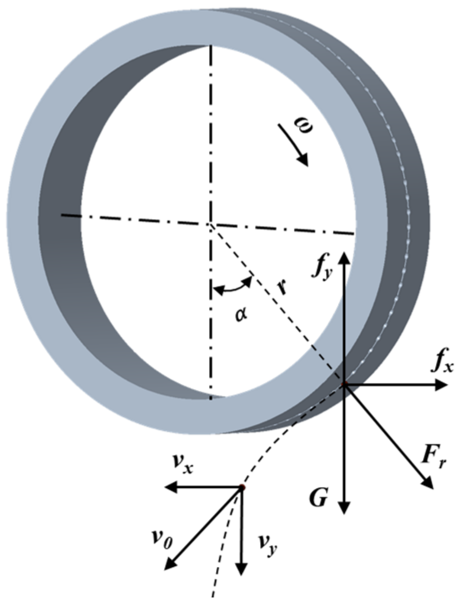

Fig. 4 - Force analysis of a seed during discharge

The initial velocity v_0 of the seed when it leaves the hole can be decomposed into horizontal and vertical components v_x and v_y. During the subsequent falling process, the seed is subjected to the combined action of gravity G, centrifugal force F_r and aerodynamic drag f. The gravity components along the x-axis and y-axis are expressed as ma_x and ma_y respectively, and the aerodynamic drag f is also decomposed into f_x and f_y accordingly. Thus, the equilibrium equations are obtained as follows:

$$\begin{cases} ma_x = -f_x - F_r \sin\alpha \\ ma_y = -F_r \cos\alpha - f_y \\ F_r = m\omega^2 r \end{cases} \tag{5}$$

where: m is the mass of a single seed, [kg]; α is angle between centrifugal direction of a single seed and vertical direction, [rad]; a_x is tangential acceleration of a single seed, [m/s²]; a_y is normal acceleration of a single seed, [m/s²]; r is distance from seed centroid to center of seed metering wheel, [m]; ω is angular velocity of seed metering wheel, [rad/s].

Rapeseed grains are small in size, light in weight, and fall over a short distance, so the effect of the drag force can be neglected. The movement of seeds during the seeding stage can be simplified as projectile motion. Decompose the movement into horizontal displacement x and vertical displacement y, the total displacement is denoted by Z, and the time elapsed during the seeding process is denoted by t.

The relationship among them can be expressed as follows:

$$\begin{cases} Z = \sqrt{x^2 + y^2} \\ v_0 = \omega r \\ v_x = v_0 \cos \alpha \\ x = v_x t \\ y = \frac{1}{2} g t^2 \end{cases} \tag{6}$$

From Equation (6):

$$Z = \sqrt{(\omega r t)^2 + \frac{1}{4} g^2 t^4} \tag{7}$$

According to Equation (7), the movement path of seeds depends on the angular velocity ω and the rotating radius r. Since the seed diameter is much smaller than the radius of the seed metering wheel, r can be approximated as the radius of the seed metering wheel. Reducing the values of ω and r can shorten the movement distance of seeds, thereby reducing the time required in the seed-dropping stage. With reference to the design of other cell-wheel seed-metering devices *(Cong, 2014)*, the radius of the seed-metering wheel was set to 80 mm. Because the angular velocity ω affects the seed-discharge speed, it should be kept as low as possible while still ensuring the required operating efficiency.

Experimental Conditions

The experiment was conducted at the test site of Yunma Agricultural Machinery Manufacturing Co., Ltd. in Yancheng, Jiangsu Province. The rapeseed cultivar used was Ningza 1838, with a seed diameter of 2–3 mm and a 1,000-seed weight of 4.1 g. The developed precision rapeseed seed-metering device was installed in place of the original precision rice seed-metering device on a 2BLY-280B rice seedling-production line (Fig. 6). Rigid plastic trays with overall dimensions of 560 mm × 280 mm × 30 mm (length × width × height) were used. To facilitate clearer counting of the rapeseed seeds during the experiment, quicklime powder was used in place of the seedling substrate employed in actual production.

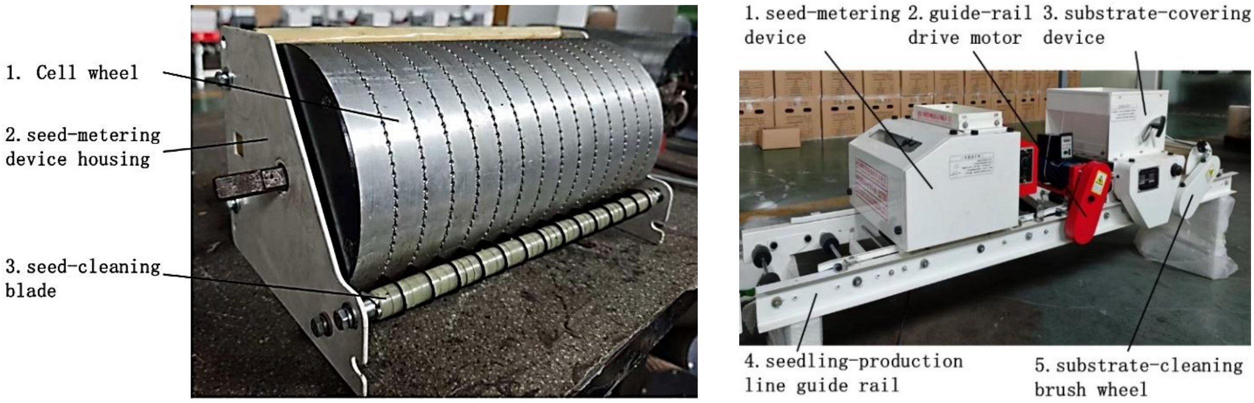

Fig. 5 - Seeder bench-test setup

According to the agronomic requirements for rapeseed mat-type seedling production *(National Technical Committee for Agricultural Machinery Standardization, 2021)*, 2–3 seeds per tray cell are considered appropriate. With reference to the relevant promotion and evaluation guidelines *(Ministry of Agriculture and Rural Affairs of the People's Republic of China, 2024)*, the qualified seed-metering rate and empty-cell rate were calculated using Equation (7). During each test, the operating parameters were adjusted and 10 consecutive trays were sown. After stable operation was achieved, the middle five trays were selected for evaluation. For each tray, five sampling areas were selected using the five-point sampling method, with 20 cells examined in each area, resulting in a total of 100 cells per tray.

The sampling method is shown in Figure 6.

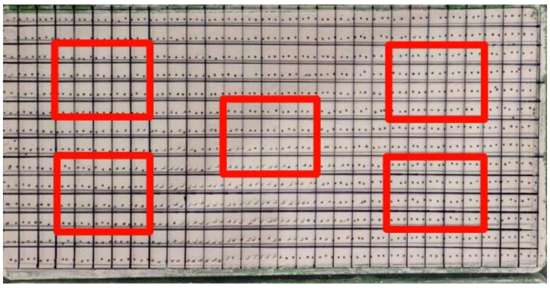

Fig. 6 - Sampling areas for seed counting in the seedling tray

The seed-metering performance indices were calculated as follows:

$$\begin{cases} R_j(\%) = \frac{H_j}{Z_j} \times 100 \\ R_K(\%) = \frac{N_k}{Z_k} \times 100 \end{cases} \tag{8}$$

where:

R_j is the qualified seed-metering rate, [%]; H_j is the number of qualified cells; Z_j is the total number of cells evaluated; R_k is the empty-cell rate, [%];N_k is the number of empty cells; Z_k is the total number of cells evaluated.

Single-factor experimental design

Based on previous studies *(Liu et al., 2025; Yu et al., 2025; Zhou et al., 2016)*, the rotational speed of the seed-metering wheel, the conveying speed of the seedling tray, and the seed-box opening size were selected as the experimental factors. Their effects on the qualified seed-metering rate and empty-cell rate were investigated. Each test was repeated five times, and the mean value was used for analysis. (1) With the seedling-tray conveying speed fixed at 0.45 $m \cdot s^{-1}$ and the seed-box opening size fixed at 17 mm, the rotational speed of the seed-metering wheel was set to 7.6, 8.4, 9.2, 10.0, and 10.8 $r \cdot min^{-1}$. The qualified seed-metering rate and empty-cell rate were then measured. (2) With the rotational speed of the seed-metering wheel fixed at 9.2 $r \cdot min^{-1}$ and the seed-box opening size fixed at 17 mm, the seedling-tray conveying speed was set to 0.35, 0.40, 0.45, 0.50, and 0.55 $m \cdot s^{-1}$ to evaluate its effect on seed-metering performance. (3) With the rotational speed of the seed-metering wheel fixed at 9.2 $r \cdot min^{-1}$ and the seedling-tray conveying speed fixed at 0.45 $m \cdot s^{-1}$, the seed-box opening size was set to 10, 13.5, 17, 20.5, and 24 mm for testing.

Effects of Seed-Metering Wheel Speed on Seeding Performance

As shown in Fig. 7, as the rotational speed of the seed-metering wheel increased, the qualified seed-metering rate initially increased and then decreased, whereas the empty-cell rate showed the opposite trend. This was mainly because an increase in rotational speed enhanced the mobility of the seed mass and strengthened the entrainment effect of the seed-metering wheel on the seeds, thereby facilitating seed entry into the cells and significantly reducing the empty-cell rate. The resulting improvement in seed-filling efficiency also increased the qualified seed-metering rate, indicating the presence of a relatively stable seed-filling range at intermediate rotational speeds. However, an excessively high rotational speed shortened the effective contact time between the seeds and the cells. Consequently, the seed-filling process could not be completed before the seeds were carried away from the seed bed. At the same time, the centrifugal effect became more pronounced, causing some seeds to leave the cells because of inertia. This resulted in insufficient filling, an increase in the empty-cell rate, and a decrease in the qualified seed-metering rate. Therefore, to maintain a qualified seed-metering rate above 90% while keeping the empty-cell rate within an acceptable range, the rotational speed of the seed-metering wheel should be set to 8.4–10 $r \cdot min^{-1}$.

Effects of Seedling-Tray Conveying Speed on Seed-Metering Performance

As shown in Fig. 8, as the seedling-tray conveying speed increased, the qualified seed-metering rate initially increased and then decreased, whereas the empty-cell rate showed the opposite trend. Within the low-to-medium speed range, an increase in conveying speed improved the coordination between seed discharge and tray movement, allowing the discharged seeds to enter the tray cells more accurately. This reduced missed seeding, sharply decreased the empty-cell rate, improved seed-distribution uniformity, and significantly increased the qualified seed-metering rate. When the conveying speed exceeded the critical value of 0.45 m·s^{-1}, two adverse effects occurred. First, the impact velocity of the seeds upon contact with the substrate in the seedling tray increased, resulting in seed bouncing and scattering and thereby reducing seeding uniformity. Second, the time interval during which each tray cell passed beneath the seed-discharge position became too short for the seeds to settle stably in the cells, leading to an increase in the empty-cell rate. Therefore, considering both seed-metering performance and production efficiency, a seedling-tray conveying speed of 0.40–0.50 m·s^{-1} was considered appropriate.

Effects of Seed-Box Opening Size on Seed-Metering Performance

As shown in Fig. 9, the qualified seed-metering rate decreased when the seed-box opening size increased from 10 to 13.5 mm, increased when the opening size increased from 13.5 to 17 mm, and then gradually decreased when the opening size exceeded 17 mm. The rate of decrease became smaller when the opening size exceeded 20.5 mm. The empty-cell rate initially decreased and then increased. As the seed-box opening size increased, the quantity of seeds entering the seed-filling zone also increased, producing two beneficial effects. First, increased interseed friction reduced the mobility of the seed mass and limited seed bouncing during the seed-filling process. Second, the increased pressure within the seed mass promoted more complete filling of the cells. However, when the opening size exceeded the critical value of 17 mm, excessive seed accumulation increased interseed compression and friction, potentially causing seed jamming and disrupting seed-metering uniformity. In addition, excessive seed accumulation in the seed passage prevented some cells from being completely filled. Therefore, the seed-box opening size was selected within the range of 10–24 mm.

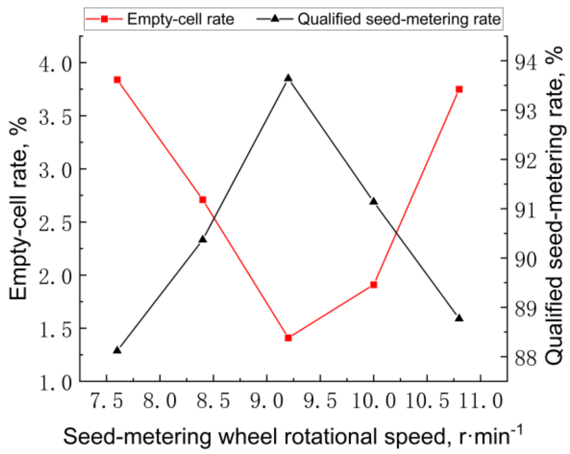

Fig. 7 - Effects of seed-metering wheel rotational speed on seed-metering performance

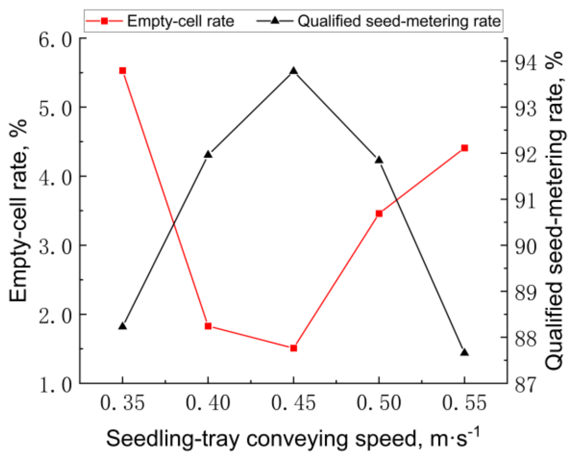

Fig. 8 - Effects of seedling-tray conveying speed on seed-metering performance

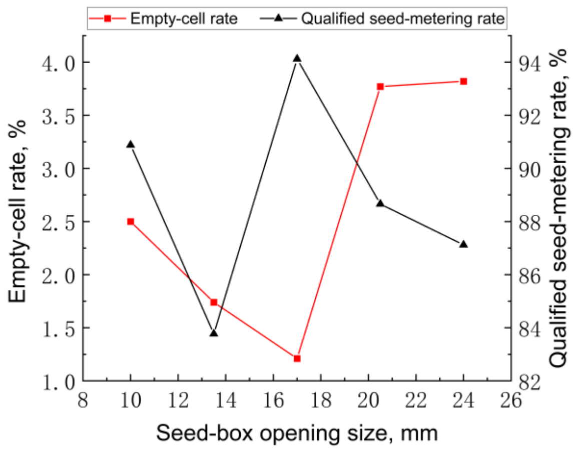

Fig. 9 - Effects of seed-box opening size on seed-metering performance

Experimental design

Based on the factor ranges determined from the single-factor experiments, a three-factor, three-level orthogonal experiment was conducted using the qualified seed-metering rate (R_j) and empty-cell rate (R_k) as the evaluation indices. The experimental factors and their levels are listed in Table 2. X_1, X_2 and X_3 represent the coded values of the seed-metering wheel rotational speed, seedling-tray conveying speed, and seed-box opening size, respectively. A total of 17 experimental runs were performed. Each run was repeated three times, and the mean value was used for analysis. The experimental results are presented in Table 3.

Table 2

Experimental factors and levels

Level	Seed-metering wheel rotational speed X_1 [r·min^{-1}]	Seedling-tray conveying speed X_2 [m·s^{-1}]	Seed-box opening size X_3 [mm]
-1	8.4	0.4	10
0	9.2	0.45	17
1	10	0.5	24

RESULTS

The experimental results are presented in Table 3. Regression analysis of the experimental data was performed using Design-Expert 13.0, and the following regression equations were obtained:

$$R_j = 93.78 - 0.39X_1 + 0.2662X_2 + 1.63X_3 - 0.75X_1X_2 + 0.04X_1X_3 + 0.7075X_2X_3 - 2.21X_1^2 - 2.86X_2^2 - 1.35X_3^2 \quad (9)$$

$$R_k = 1.58 + 0.9963X_1 - 0.345X_2 - 0.7138X_3 - 0.49X_1X_2 + 0.3025X_1X_3 + 0.295X_2X_3 + 1.22X_1^2 + 0.8123X_2^2 + 0.1847X_3^2 \quad (10)$$

The analysis of variance presented in Table 4 showed that both regression models were highly significant (P < 0.01), whereas the lack-of-fit terms were not significant (P > 0.05), indicating that the models adequately fitted the experimental data. The coefficients of determination, R^2, were 0.9985 and 0.9821 for the qualified seed-metering rate and empty-cell rate models, respectively. The corresponding adjusted R^2 values were 0.9966 and 0.9591, and the predicted R^2 values were 0.9942 and 0.7657. The coefficients of variation were 0.1571% and 9.64%, respectively. These results indicate good agreement between the predicted and experimental values. The order of influence of the experimental factors on seed-metering performance was seed-box opening size, followed by seedling-tray conveying speed and seed-metering wheel rotational speed.

Table 3

Results of the response-surface experiment

Test No.	Seedling-tray conveying speed X_2 [m·s^{-1}]	Seed-metering wheel rotational speed X_1 [r·min^{-1}]	Seed-box opening size X_3 [mm]	Empty-cell rate R_k [%]	Qualified seed-metering rate R_j [%]
1	0.45	8.4	10	3.82	88.31
2	0.4	8.4	17	2.42	88.09
3	0.5	9.2	24	3.41	91.45
4	0.45	8.4	24	1.78	90.27
5	0.45	9.2	17	1.54	93.97
6	0.45	9.2	17	1.82	93.51
7	0.45	10	10	2.78	87.44
8	0.4	9.2	10	3.17	89.07
9	0.45	9.2	17	1.42	93.75
10	0.4	9.2	24	1.16	92.15
11	0.5	9.2	10	4.21	88.21
12	0.45	10	24	1.92	92.23
13	0.45	9.2	17	1.51	93.81
14	0.5	10	17	3.83	87.83
15	0.4	10	17	2.47	90.11
16	0.5	8.4	17	5.74	88.81
17	0.45	9.2	17	1.6	93.87

Note: *Each treatment was replicated three times, and the reported values are the means.*

The analysis of variance indicated interaction effects among the seed-metering wheel rotational speed, seedling-tray conveying speed, and seed-box opening size. The corresponding response surfaces are shown in Fig.10.

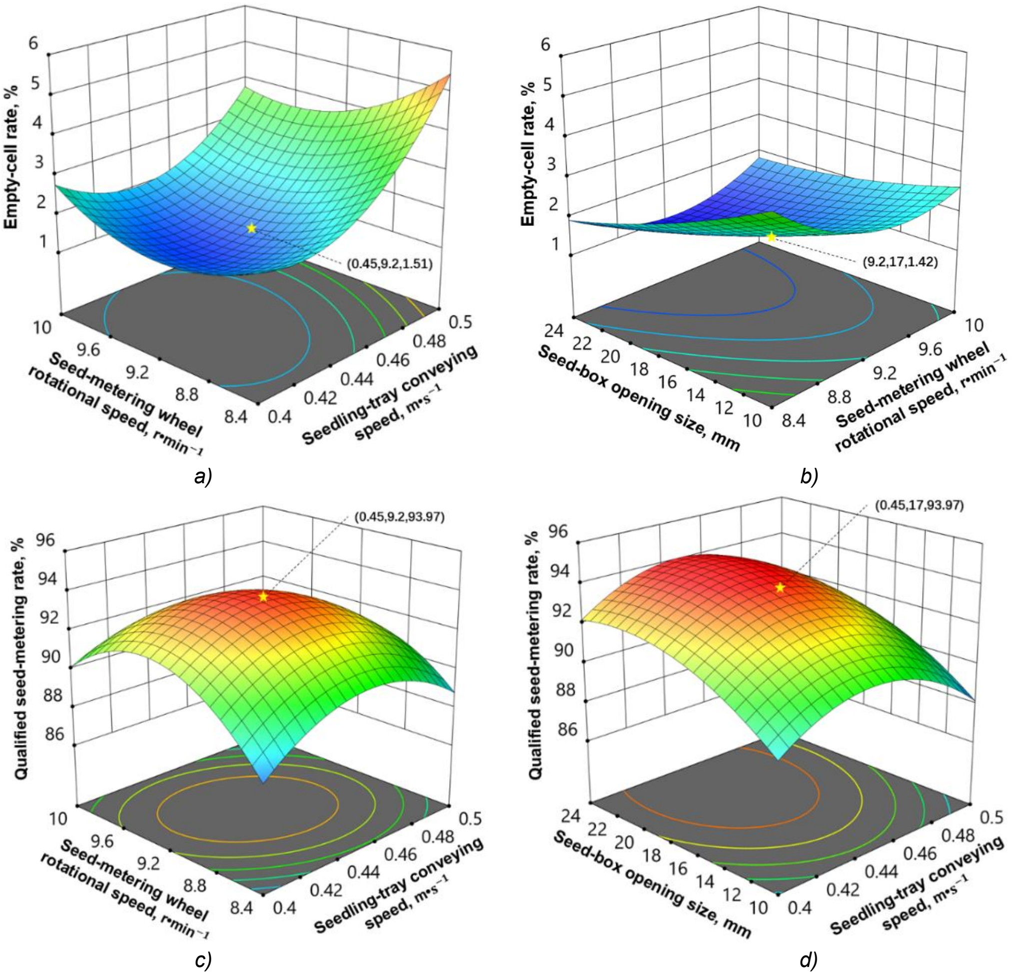

Fig. 10 - Response surfaces showing the interactive effects of seed-metering wheel rotational speed, seedling-tray conveying speed, and seed-box opening size on the qualified seed-metering rate and empty-cell rate

The interaction between X_1 and X_2 reflects the temporal and spatial coordination between the seed-discharge frequency and the rate at which tray cells pass beneath the discharge position (Figs. 10a and 10b). At low values of both X_1 and X_2, seed agitation and circulation in the filling zone are relatively weak, resulting in insufficient cell filling (Eq. 2). Meanwhile, the low rotational speed of the seed-metering wheel produces a low initial seed-release velocity, and the horizontal displacement of the seed during flight, (Eq. 6), remains relatively small. As both factors increase toward their intermediate levels, the seed-discharge frequency becomes better matched to the tray-cell passing frequency, allowing the seeds to land more accurately in the tray cells. This region therefore represents the optimal synchronization range, in which the qualified seed-metering rate reaches its maximum. When X_2 is high while X_1 remains low, the seed supply rate per unit time may be insufficient relative to the number of tray cells passing beneath the discharge position, resulting in a marked increase in the empty-cell rate. This represents a temporal mismatch between seed supply and tray-cell demand. Conversely, when X_1 is high while X_2 is low, seeds are discharged with greater initial velocity ($v_y = gt$) and may undergo increased bouncing or scattering after striking the substrate, thereby reducing the qualified seed-metering rate even when the seed supply is sufficient. The deterioration in performance at the highest combination of the two factors is attributed to the excessive rotational speed of the seed-metering wheel ($Fc>mg$), which may cause seeds to detach prematurely from the cells before reaching the optimal discharge position (Eq. 5). This leads to irregular landing positions and a sharp increase in the empty-cell rate.

The interaction between X_1 and X_3 reflects the balance between the available seed-filling time and the pressure exerted by the seed mass at the cell entrance (Figs. 10c and 10d). At a small seed-box opening size (low X_3), the quantity of seeds entering the filling zone is limited, and the pressure exerted by the seed layer above the cells is relatively low. As X_1 increases, the effective seed-filling time decreases proportionally (Eq. 4), making it more difficult for seeds to enter the cells completely. Consequently, the qualified seed-metering rate decreases rapidly at small opening sizes. Increasing X_3 increases the amount of seed in the filling zone and enhances both interseed contact and the pressure exerted by the upper seed layer. Within an appropriate range, this promotes seed entry into the cells and improves the qualified seed-metering rate. However, when the opening size exceeds a critical value, approximately 17 mm according to the response-surface results, excessive seed accumulation may increase interseed compression and restrict the mobility of the seed mass. This can promote bridging or arching near the cell entrances, thereby obstructing seed flow and reducing the effective filling rate. The ridge observed in the response surface therefore indicates that an optimal combination of rotational speed and seed-box opening size is required: sufficient seed pressure is needed to promote filling, but excessive accumulation should be avoided to prevent flow obstruction. The gradual decline observed when the opening size exceeded 20.5 mm in the single-factor experiment shown in Fig. 9 may also be associated with this reduced seed mobility and localized bridging. Although the X_2X_3 interaction term was not significant for the qualified seed-metering rate (P=0.5922 , Table 4), it was significant for the empty-cell rate (P=0.0480).

The seedling-tray conveying speed X_2 affects the relative horizontal position between the falling seeds and the moving tray cells, whereas the seed-box opening size X_3 influences the quantity of seeds supplied to the discharge zone. At a high conveying speed, the available time for each tray cell to pass beneath the discharge position is reduced, increasing the likelihood of positional misalignment. A larger seed-box opening size increases the seed flow rate and may intensify interseed collisions, bouncing, and scattering during discharge. Therefore, at higher conveying speeds, a moderately smaller opening size may help limit excessive seed flow and reduce collision-induced scattering. This interpretation is consistent with the slight shift in the optimal region observed in the response surface as X_2 increased from 0.4 to 0.5 $m \cdot s^{-1}$.

Table 4

Analysis of variance for the regression models

Source of variance	Analysis of Variance of Void Rate				Analysis of Variance of Qualified Rate			
	Sum of squares	Degree of freedom	F	P	Sum of squares	Degree of freedom	F	P
Model	24.58	9	42.69	<0.0001	96.77	9	528.91	<0.0001
X_2	7.94	1	124.12	<0.0001	1.22	1	59.85	0.0001
X_1	0.9522	1	14.88	0.0062	0.5671	1	27.90	0.0011
X_3	4.08	1	63.71	<0.0001	21.35	1	1050.36	<0.0001
X_2X_1	0.9604	1	15.01	0.0061	2.25	1	110.68	<0.0001
X_2X_3	0.3660	1	5.72	0.0480	0.0064	1	0.3148	0.5922

Source of variance	Analysis of Variance of Void Rate				Analysis of Variance of Qualified Rate			
	Sum of squares	Degree of freedom	F	P	Sum of squares	Degree of freedom	F	P
$X_1 X_3$	0.3481	1	5.44	0.0524	2.00	1	98.49	<0.0001
X_2^2	6.32	1	98.73	<0.0001	20.51	1	1009.06	<0.0001
X_1^2	2.78	1	43.42	0.0003	34.55	1	1699.76	<0.0001
X_3^2	0.1437	1	2.25	0.1776	7.73	1	380.13	<0.0001
Residual	0.4478	7			0.1423	7		
Lack of fit	0.3577	3	5.29	0.0706	0.0234	3	0.2627	0.8495
Pure error	0.0901	4			0.1189	4		
Total	25.03	16			96.91	16		

Note: P ≤ 0.01 indicates the model is highly significant, 0.01 < P ≤ 0.05 indicates the model is significant, and P > 0.05 indicates the model is not significant.

Each response surface was constructed using the mean of three replicate measurements for each treatment combination listed in Table 3. The red asterisk (★) in each subfigure indicates the optimal operating point identified through multi-objective optimization.

Optimization and Verification

Using the optimization module in Design-Expert 13.0, multi-objective optimization was performed to minimize the empty-cell rate and maximize the qualified seed-metering rate. During the numerical optimization, the seedling-tray conveying speed (X_2) was fixed at 0.45 m·s⁻¹ for the following reasons: (i) this value corresponded to the optimal performance range identified in the single-factor experiment (Fig. 8) and was also consistent with the standard operating speed of commercial seedling-production lines, thereby ensuring compatibility with upstream and downstream operations; (ii) in practical production, the conveying speed is determined by the overall cycle time of the production line and is rarely adjusted during operation, whereas the seed-metering wheel rotational speed and seed-box opening size are the main parameters adjusted by operators to improve seed-metering quality; and (iii) fixing X_2 at its optimal value allowed the optimization to focus on the two most influential and practically adjustable factors, X_1 *and* X_3, thereby producing results that could be applied directly without changing the operating speed of the entire production line. Accordingly, the optimization objectives and constraints were defined as follows:

$$\begin{cases} minY_1(x1, x2, x3) \\ maxY_2(x1, x2, x3) \\ s.t.\begin{cases} 8.4 \leqslant x_1 \leqslant 10 \\ x_2 = 0.45 \\ 10 \leqslant x_3 \leqslant 24 \end{cases} \end{cases} \tag{10}$$

The optimal parameter combination obtained through numerical optimization was a seed-metering wheel rotational speed of 9.16 r·min⁻¹, a seedling-tray conveying speed of 0.45 m·s⁻¹, and a seed-box opening size of 22.80 mm. Under these conditions, the predicted qualified seed-metering rate and empty-cell rate were 94.15% and 1.12%, respectively. Three replicate bench verification tests were conducted using the optimal parameter combination. The measured mean qualified seed-metering rate was 94.41%, with a standard deviation of 0.23 percentage points and a 95% confidence interval of 93.85%–94.97%. The measured mean empty-cell rate was 1.49%, with a standard deviation of 0.036 percentage points and a 95% confidence interval of 1.40%–1.58%. The predicted qualified seed-metering rate of 94.15% and empty-cell rate of 1.12% both fell within the corresponding 95% confidence intervals of the measured values. The absolute deviations between the predicted and measured values were 0.26 and 0.37 percentage points, respectively, both of which were below the engineering tolerance threshold of 0.5 percentage points. The optimal parameter combination obtained through optimization was a seed-metering wheel rotational speed of 9.16 r·min⁻¹, a seedling-tray conveying speed of 0.45 m·s⁻¹, and a seed-box opening size of 22.80 mm. The predicted qualified seed-metering rate was 94.15%, and the predicted empty-cell rate was 1.12%. Subsequently, a bench verification experiment was conducted using this parameter combination. The experiment was repeated five times, and the mean qualified seed-metering rate and empty-cell rate were 94.41% and 1.49%, respectively. These results demonstrate that the regression models provide adequate predictive accuracy and reliability for practical operation.

CONCLUSIONS

(1) This study extends beyond parameter optimization by clarifying the underlying seed-filling and seed-discharge mechanisms of a cell-wheel seed-metering device designed for rapeseed blanket seedling production. Seed-metering performance was governed by three interacting mechanisms: the competition between the available seed-filling time and premature seed release, which was mainly affected by the seed-metering wheel rotational speed; the transition between pressure-assisted filling and seed bridging, which was mainly affected by the seed-box opening size; and the trade-off between landing accuracy and seed bouncing, which was mainly affected by the seedling-tray conveying speed. The cylindrical cells, with a diameter of 3 mm and a depth of 5 mm, together with the coordinated action of the seed-cleaning brush and blade, reduced cell blockage and seed damage and enabled stable metering of 2–3 seeds per tray cell.

(2) The validated regression models provided reliable predictions of seed-metering performance, with R^2 values of 0.9985 for the qualified seed-metering rate and 0.9821 for the empty-cell rate. The absolute deviations between the predicted and measured values were below 0.5 percentage points. The optimal parameter combination consisted of a seed-metering wheel rotational speed of 9.16 $r \cdot min^{-1}$, a seedling-tray conveying speed of 0.45 $m \cdot s^{-1}$, and a seed-box opening size of 22.80 mm. Because the optimization was conducted at the standard operating speed of the seedling-production line, the resulting parameter combination can be applied directly in practical operation. Factor significance order was: seed box opening > tray speed > metering wheel speed.

(3) This study has three main limitations. First, quicklime powder was used instead of the actual seedling substrate during the bench tests, which may have affected seed landing and bouncing behavior. Second, only the Ningza 1838 rapeseed cultivar was evaluated; therefore, other cultivars may require recalibration of the operating parameters. Third, the seedling-tray conveying speed was fixed during numerical optimization, and adaptive adjustment of the conveying speed was not investigated. Future research should include production-scale or field validation using actual seedling substrate, testing of multiple rapeseed cultivars, and the development of a closed-loop control system for adaptive parameter adjustment.

ACKNOWLEDGEMENT

The authors were funded for this project by the national key R & D project, 2023YFD2001001 and China Agriculture Research System of MOF and MARA（CARS-12）.

REFERENCES

[1] Albasheer A.H., Liao Q., Wang L., Anas D. A., Lin J., (2024). Design and preliminary evaluation of a precision cylindrical air-assisted drill sowing device for rapeseed, wheat, and rice. *Agriculture*, Vol. 14, no. 12, pp.2355, Switzerland. DOI: https://doi.org/10.3390/agriculture14122355

[2] Akhalaya B.K., Shogenov Y.K., Starovoitova S.I., (2021). Effect of design changes in pneumatic seeding devices on quality indicators of seeding. *Russian Agricultural Sciences*, Vol. 47, no.1, pp.93–98, Moscow/Russia. DOI: https://doi.org/10.3103/S106836742101002X

[3] Cong J., (2014). *Study on Seeding System and Mechanism of Pneumatic Precision Metering Device for Wheat & Rapeseed (油菜小麦兼用型气力式精量排种系统及其机理研究)*. PhD dissertation, Huazhong Agricultural University, Wuhan/China.

[4] Cao X., Ma X., Li H., Wen Z., Li Z., Wang X., (2021). Design and experiments of pneumatic roller type precision seed-metering device for rapeseed plug seedlings (气吸滚筒式油菜穴盘育苗精密排种器设计与试验). *Transactions of the Chinese Society of Agricultural Engineering*, Vol. 37, no. 2, pp. 51-60, Beijing/China. DOI: https://doi.org/10.11975/j.issn.1002-6819.2021.2.007

[5] Chinese Academy of Agricultural Mechanization Sciences., (2007). *Agricultural Machinery Design Manual,* Vol 1 & Vol 2, Agricultural Science and Technology Press, ISBN9787802333352, Beijing/China.

[6] Deng C., (2023). *Development and Testing of a Centralized Rapeseed Seeding and Fertilizing Device (集排式油菜播种施肥装置研制与试验)*. Msc Thesis, Southwest University, Chongqing/China.

[7] Gao L., Shi B., Liao Q., Zhang B., Zheng J., Liao Y., (2022). Seeding performance of conical-hole seeding plate of the positive and negative pressure combination precision seed metering device for rapeseed (正负气压组合油菜精量排种器锥孔盘排种性能). *Transactions of the Chinese Society of*

Agricultural Engineering, Vol. 38, no. 6, pp. 22-33, Beijing/China. DOI: https://doi.org/10.11975/j.issn.1002-6819.2022.06.003

[8] Jiang L., Zhu T., Tang Q., Wu J., Jiang D., Huang M., (2024). Mechanical Characteristics Testing and Parameter Optimization of Rapeseed Blanket Seedling Conveying for Transplanters. *Agriculture*, Vol 14, no.5, pp. 699, Switzerland. DOI: https://doi.org/10.3390/agriculture14050699

[9] Karayel D., Güngör O., Šarauskis E., (2022). Estimation of optimum vacuum pressure of air-suction seed-metering device of precision seeders using artificial neural network models. *Agronomy*, Vol. 12, no. 7, pp. 1600, Switzerland. DOI: https://doi.org/10.3390/agronomy12071600

[10] Lin G., Wang L., Li J., Qian C., Li Y., Zheng J., You J., Zuo Q., (2023). Research progress on mechanized transplantation technology of rapeseed blanket seedlings (油菜毯苗机械化移栽技术研究进展). *Jiangsu Agricultural Sciences*, Vol. 51, no. 18, pp. 20-27, Nanjing/China. DOI: https://doi.org/10.15889/j.issn.1002-1302.2023.18.003

[11] Li Z., Yang W., Wu Y.Y., He S., Wang W., Chen L., (2020). Performance analysis and experiments of seed filling assisted by groove-tooth of pneumatic disc precision metering device for rapeseed (油菜气力盘式精量排种器槽齿辅助充种性能分析与试验). *Transactions of the Chinese Society of Agricultural Engineering*, Vol. 36, no. 20, pp. 57-66, Beijing/China. DOI: https://doi.org/10.11975/j.issn.1002-6819.2020.20.008

[12] Liao Y., Liao Q., Wang L., Zheng J., Gao L.P., (2018). Investigation on vacuum singulating effect influencing factors of pneumatic precision seed metering device for small particle size of seeds (气力式小粒径种子精量排种器吸种效果影响因素研究). *Transactions of the Chinese Society of Agricultural Engineering*, Vol. 34, no. 24, pp.10-17, Beijing/China. DOI: https://doi.org/10.11975/j.issn.1002-6819.2018.24.002

[13] Li Z., Yang W., Zhang T., Wang W., Zhang S, Chen L., (2019). Design and suction performance test of sucking-seed plate combined with groove-tooth structure on high speed precision metering device of rapeseed (油菜高速精量排种器槽齿组合式吸种盘设计与吸附性能试验). *Transactions of the Chinese Society of Agricultural Engineering*, Vol. 35, no. 1, pp. 12-22, Beijing/China. DOI: https://doi.org/10.11975/j.issn.1002-6819.2019.01.002

[14] Li P., Gu Y., Zhang T., Feng W., Ren G., Zhou X., Wu M., (2025). Design and Experiment of Inclined Disc Precision Seeding Apparatus for Rape (倾斜圆盘式油菜精密排种器设计与试验). *Journal of Agricultural Mechanization Research*, Vol. 47, no. 09, pp. 178-186, Haerbin/China. DOI: https://doi.org/10.13427/j/issn.1003-188x.2025.09.024

[15] Liu Y., Wu Z., Nie Y., Liu F., Wu M., (2019). Seeding performance of double hole-wheel seeder for rapeseed based on EDEM (基于 EDEM 的双排型孔轮式油菜排种器的排种性能分析). *Journal of Hunan Agricultural University (Natural Sciences)*, Vol. 45, no. 2, pp. 554-559, Changsha/China. DOI: https://doi.org/10.13331/j.cnki.jhau.2019.05.018

[16] Liu D., Qin F., Wang Z., Xie F., Li X., Gong M., (2025). Optimization design and experiment of herringbone groove seed metering unit for rice seedling raising (人字纹斜槽式水稻育秧播种排种器优化设计与试验). *Journal of Shenyang Agricultural University*, Vol. 56, no. 2, pp. 99-109, Shenyang/China. DOI: https://doi.org/10.3969/j.issn.1000-1700.2025.02.011

[17] Lei X., Yang W., Yang L., Liu L., Liao Q., Ren W., (2020). Design and Experiment of Seed Hill-seeding Centralized Metering Device for Rapeseed (油菜精量穴播集中排种装置设计与试验). *Transactions of the Chinese Society for Agricultural Machinery*, Vol. 51, no. 2, pp. 54-64, Beijing/ China. DOI: https://doi.org/10.6041/j.issn.1000-1298.2020.02.007

[18] Ministry of Agriculture and Rural Affairs of the People's Republic of China., (2024). *Complete sets of equipment for seedling tray seeding,* DG/T 074—2024, Beijing/ China.

[19] Maleki M.R., Jafari J.F., Raufat M.H., Baerdemaeker D., (2006). Evaluation of seed distribution uniformity of a multi-flight auger as a grain drill metering device. *Biosystems Engineering*, Vol. 94, no. 4, pp. 535-543, San Diego/USA. DOI: https://doi.org/10.1016/j.biosystemseng.2006.04.003

[20] National Technical Committee for Agricultural Machinery Standardization., (2021). *Operating quality of rapeseed blanket seedling transplanter,* NY/T 3887-2021, Beijing/China.

[21] Singh R.C., Singh G., Saraswat D.C., (2006). Optimisation of design and operational parameters of a pneumatic seed metering device for planting mustard seeds. *International Agriculture Engineering Journal*, Vol. 15, no. 2, pp. 31-41, Beijing/China.

[22] Singh R.C., Singh G., Saraswat D.C., (2007). Optimisation of design and operational parameters of a pneumatic seed metering device for planting of groundnut (Arcahis hypogaea) seeds. *Indian Journal of Agricultural Sciences*, Vol. 77, no. 1, pp. 40-42, New Delhi/India.

[23] Singh R.C., Singh G., Saraswat D.C., (2005). Optimisation of design and operational parameters of a pneumatic seed metering device for planting cottonseeds. *Biosystems Engineering*, Vol. 92, no. 4, pp. 429–438, San Diego/USA.DOI: https://doi.org/10.1016/j.biosystemseng.2005.07.002

[24] Wu C., Wang J., Yang Y., Li D., Li X., Yan R., (2024). Analysis of the development status and mechanization trends of economic crop industry in China (我国经济作物产业发展现状与机械化趋势分析). *Journal of Chinese Agricultural Mechanization*, Vol. 45, no.1, pp. 01-13, Nanjing/China. DOI: https://doi.org/10.13733/j.jcam.issn.2095-5553.2024.01.001

[25] Wang Z., Leng S., Zhang Y., Zhou X., Gong C., Zuo Q., Yang G., (2023). Research progress on seedling transplanting technology of rapeseed blanket-like seedlings (油菜毯状苗育苗移栽技术研究进展). *Jiangsu Journal of Agricultural Sciences*, Vol.39, no. 5, pp. 1247-1255, Nanjing/China. DOI: https://doi.org/10.3969/j.issn.1000-4440.2023.05.018

[26] Wang B., Wang L., Liao Y., Wu C., Cao M., Liao Q., (2022). Design and Test of Seeding Wheels of Precision Hole-seeding Centralized Metering Device for Small Particle Size Seeds (小粒径种子精量穴播集排器型孔轮设计与试验). *Transactions of the Chinese Society for Agricultural Machinery*, Vol. 53, no. 11, pp. 64-75, 119, Beijing/China. DOI: https://doi.org/10.6041/j.issn.1000-1298.2022.11.007

[27] Wu J., Yu W., Zhang M., Wu C., Jiang L., Tang Q., (2020). Design and Test of 2ZY-6 Rapeseed Carpet Seedling Transplanter (2ZY-6 型油菜毯状苗移栽机设计与试验). *Transactions of the Chinese Society for Agricultural Machinery*, Vol 51, no. 12, pp. 95-102, 275, Beijing/China. DOI: https://doi.org/10.6041/j.issn.1000-1298.2020.12.010

[28] Xing H., Liao Q., Wang L., Wang D., Liao Y., Wang D., Yu Q., (2019). Design and test of oblique taper hole-type wheel centralized metering device for rapeseed and wheat (油麦兼用斜锥型孔轮式集排器设计与试验). *Journal of Huazhong Agricultural University*, Vol. 38, no. 5, pp. 143-151, Wuhan/China. DOI: https://doi.org/10.13300/j.cnki.hnlkxb.20190701.003

[29] Yu Y., Pan Y., Wang T., Wang Y., Luo T., (2025). Design and Test of Drum Seed Metering Device for Drill Seeding of Rice Blanket Seedlings (播量可调式水稻毯苗条播机滚筒排种器设计与试验). *Transactions of the Chinese Society for Agricultural Machinery*, Vol. 56, no. 10, pp. 310-320, Beijing/China. DOI: https://doi.org/10.6041/j.issn.1000-1298.2025.10.026

[30] Zhang Q., Yu Q., Wang L., Liao Y., Wang D., Liao Q., (2020). Design and Experiment of Scoop-type Precision Hole Metering Device for Rapeseed (油菜勺式精量穴播排种器设计与试验). *Transactions of the Chinese Society for Agricultural Machinery*, Vol. 51, no. 6, pp. 47-54, 64, Beijing/ China. DOI: https://doi.org/10.6041/j.issn.1000-1298.2020.06.005

[31] Zhou H., Liang Q., Wei T., Ma X., Jiao C., (2016). Design and Experiment of Quantitative Seed Supply Device with Fluted Roller Used for Double-vibrating Precision Seed Meter (双级振动精密排种器外槽轮式定量供种装置设计与试验). *Transactions of the Chinese Society for Agricultural Machinery*, Vol. 47, no. s1, pp. 57-61, Beijing/China. DOI: https://doi.org/10.6041/j.issn.1000-1298.2016.S0.009